Sound Velocity Measurements of Nuclear-Ordered Solid ^{3}He along the Melting Curve

R. Nomura,* M. Yamaguchi, K. Takaoka, X. Xu, Y. Sasaki, and T. Mizusaki

Department of Physics, Graduate School of Science, Kyoto University, Kyoto 606-8502, Japan

(Received 2 June 2000)

We have measured the temperature dependence of the 10.98 MHz longitudinal sound velocity of solid ^{3}He in the nuclear-ordered $U2D2$ phase and in the paramagnetic phase along the melting curve. The temperature dependence of the sound was attributed to the contributions from the nuclear spin system and the molar volume change along the melting curve. The sound velocity increased with temperature as T^4 in the $U2D2$ phase and the sound anisotropy due to the exchange interaction was found to be about 10% among single-domain crystals investigated. The average value of the Grüneisen constant of the spin wave velocity in the ordered phase was $\bar{\gamma}_c = 16$ and is compared to the calculated value of the multiple-exchange model.

PACS numbers: 67.80.Cx, 67.80.Jd

Nuclear spin ordering occurs by multiple-exchange interactions of the nuclear spins in solid ^{3}He. The exchange interactions depend strongly on the molar volume and thus the lattice deformation of the sound wave is coupled to the nuclear spin systems. Therefore, sound measurements are regarded to be useful for studying the nuclear magnetism of solid ^{3}He at ultralow temperatures below 10 mK, where the nuclear spin system dominates the thermodynamic quantities. Nuclear spin ordering occurs at the Néel temperature, $T_N = 0.93$ mK, on the melting pressure at zero external magnetic field and this is known as the first order transition. There are two ordered phases found in bcc solid ^{3}He under applied magnetic fields and we focused our sound measurement in the low-field phase, the so-called $U2D2$ phase [1]. Theoretical predictions of the acoustic properties of solid ^{3}He, such as the sound velocity, the attenuation, and the coupling of sound with the collective mode of nuclear spin system in the ordered phase, were discussed in Ref. [2]. However, the sound measurement reported so far was limited to 12 mK [3]. We report the first measurement of the sound velocity in the $U2D2$ phase as well as in the paramagnetic phase where the exchange contributions of nuclear spins to the velocity can be observed.

The $U2D2$ phase has a uniaxial symmetry of the nuclear spin structure and its anisotropy axis, $\mathbf{l}$, is a (100) direction of bcc crystal or other equivalent axes. A single crystal of the $U2D2$ solid ^{3}He usually has three magnetic domains, each of which has a size comparable to a whole crystal [4]. The origin of this domain structure in the antiferromagnet is not yet understood. When a crystal was grown in the superfluid B phase in the narrow tube, the upper part of the sample in the tube was dominated by a single domain [5,6]. Because of the high quality of sample which guarantees a good thermal conductivity within the sample and the very small Kapitza resistance between solid and liquid [7,8], the solid was in good thermal equilibrium with liquid at least in the ordered phase. Figure 1 is a schematic drawing of the sample cell [9]. The lower part is a narrow tube of 1 mm diameter with a heater (A) at the bottom to nucleate a seed crystal. The seed was grown in the tube and continued to grow in the space between two transducers (B) and a spacer (C). The spacer had two windows (D) patched with polyester (PET) mesh to ensure a good thermal contact with the superfluid ^{3}He. We had two NMR coils (E, F), E was used for monitoring the seed crystal, and F for monitoring the sample where we measured the sound velocity. The main magnetic field for NMR was parallel to the direction of the propagation of the sound, so that we could determine both the temperature of the crystals and the domain orientation with respect to the sound propagation from the NMR frequency shifts in the $U2D2$ phase [1]. The NMR field was about 200 G and the field dependence of the thermodynamic properties of solid ^{3}He was negligible. Above T_N the temperature of solid was determined by the melting pressure [10].

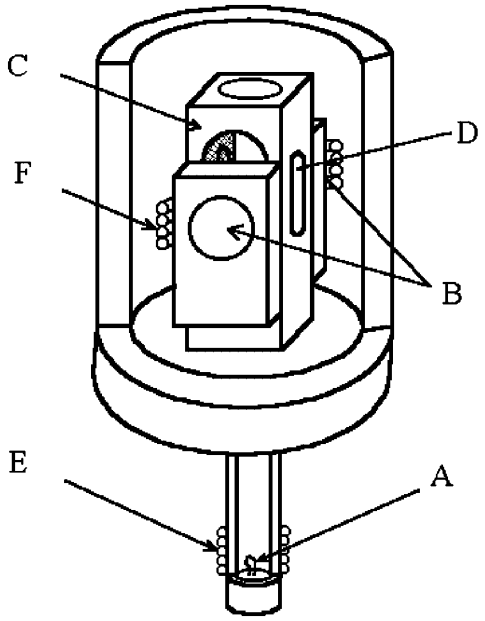

FIG. 1. Schematic view of the sample cell. A: nucleation heater; B: transducers; C: spacer; D: window; E, F: NMR coils.

We used one transducer to send sound pulses and the other as the receiver. The longitudinal sound frequency was 10.98 MHz and the sound path length was 3.1 mm. Sound echoes were detected by a phase sensitive detector and recorded by a digitizer for each pulse. Absolute values of the sound velocity were determined from the time intervals between the echo peaks. Absolute accuracy of the sound velocity was about 1%. Relative change of the sound velocity, $\Delta v/v$, was obtained by measuring the phase changes of the echo signals. The resolution of the measured velocity change after averaging about 20 data points was about 2×10^{-5}.

Attenuation of sound in good solid samples was 0.2 cm^{-1} for the entire temperature range and was attributed to the diffraction loss of our geometry of the two transducers. Therefore, this value gives the upper limit of the intrinsic attenuation of solid.

The orientation dependence of the measured sound velocities for about 20 samples agreed well with the value calculated from the reported elastic constant, c_{ij} [11,12], scaled to our molar volume by

$$\frac{d\log c_{ij}}{d\log V} = 2\gamma_L - \frac{1}{3}, \tag{1}$$

with a common Grüneisen constant for all c_{ij}, and we determined the Grüneisen constant for Debye temperature $\gamma_L = -2.35$. This value of γ_L is used for Eq. (4).

Typical overall temperature dependence of sound velocity is shown in Fig. 2. In this sample the three principal crystalline axes were (81°, 50°, and 41°) with respect to the sound propagation direction and $v = 498$ m/sec. This sample was not a single domain sample. In the $U2D2$ phase the sound velocity, $\Delta v/v$, increased with temperature by T^4. In the narrow temperature range of 0.5 mK above T_N, the velocity increased rapidly by about 0.1% and this is the velocity jump due to the first order phase transition at T_N. The temperature width of the transition above T_N was due to the slow thermal relaxation of this first order transition even though the warming-up rate of the crystal from 1 to 2 mK was 6 days. In paramagnetic phase the velocity increased slightly just above T_N, going through the maximum at around 3 mK and then decreased as the temperature increased.

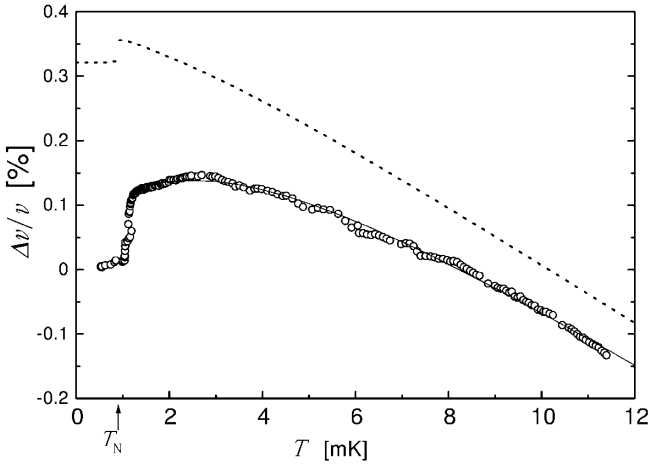

FIG. 2. Typical temperature dependence of the sound velocity. The solid line shows the fit to Eq. (3), and the dotted line is the contribution from molar volume change, Eq. (4).

We assume for analysis of data that the relaxation time within the nuclear spin system is very fast compared with the inverse of the sound frequency and the expression for the first sound is used to calculate the contribution of the nuclear spin system. The pressure of the solid, P, is calculated by the Mie-Grüneisen equation of state,

$$P = -\frac{dU_0}{dV} - \gamma U(T), \tag{2}$$

where U_0 is the total potential energy, $U(T)$ the internal energy density, V the volume, and $\gamma \equiv \frac{d\log J}{d\log V}$ the Grüneisen constant of the exchange interaction. The adiabatic bulk modulus is given by $B_S = -V(\frac{\partial P}{\partial V})_S$ and the sound velocity is calculated by using $v^2 = B_S/\rho$ for the isotropic materials, where ρ is density. Sound velocity change can be divided into two contributions,

$$\frac{\Delta v}{v} = \frac{\Delta v(V_{\mathrm{mol}})}{v} + \frac{\Delta v(T)}{v}. \tag{3}$$

The first term in Eq. (3) is due to the molar volume change along the melting curve and the second term is due to the temperature dependent energy of the nuclear spin system. The molar volume V_{mol} is known along the melting pressure [13]. The first term in Eq. (3) can be calculated as

$$\frac{\Delta v(V_{\mathrm{mol}})}{v} = \left(\gamma_L + \frac{1}{3}\right)\frac{\Delta V_{\mathrm{mol}}}{V_{\mathrm{mol}}}. \tag{4}$$

The second term in Eq. (3) is related to $U(T)$ as

$$\frac{\Delta v(T)}{v} = \frac{\Delta B_S(T)}{2B_S} = \frac{\gamma\left(\gamma - 1 - \frac{d\log\gamma}{d\log V}\right)U(T)}{2\rho v^2}, \tag{5}$$

where we assume $\frac{d\log\gamma}{d\log V} = 0$ in Eq. (5). We analyzed data separately in the three temperature regions below, at, and above T_N.

In the $U2D2$ phase below T_N, $\Delta V_{\mathrm{mol}} = -4.0 \times 10^{-4}(T/T_N)^4$ cm^3/mole [13], and

$$U(T) = \frac{\pi^2\hbar}{15c^3}\left(\frac{k_B T}{\hbar}\right)^4, \tag{6}$$

where $c = 7.8$ cm/sec [14] is the average spin wave velocity by using the Greywall temperature scale [10]. The same result as Eq. (5) with Eq. (6) was theoretically derived, assuming one common Grüneisen constant for all multiple-exchange constants [15]. Anisotropy effects in sound velocity are not included in the analysis. Temperature dependences of the spin wave contribution to the sound velocity, $\Delta v(T)/v$, in the $U2D2$ phase for four different single-domain samples are shown in Fig. 3(a), where $\Delta v(V_{\mathrm{mol}})/v$ estimated from Eq. (4) is subtracted

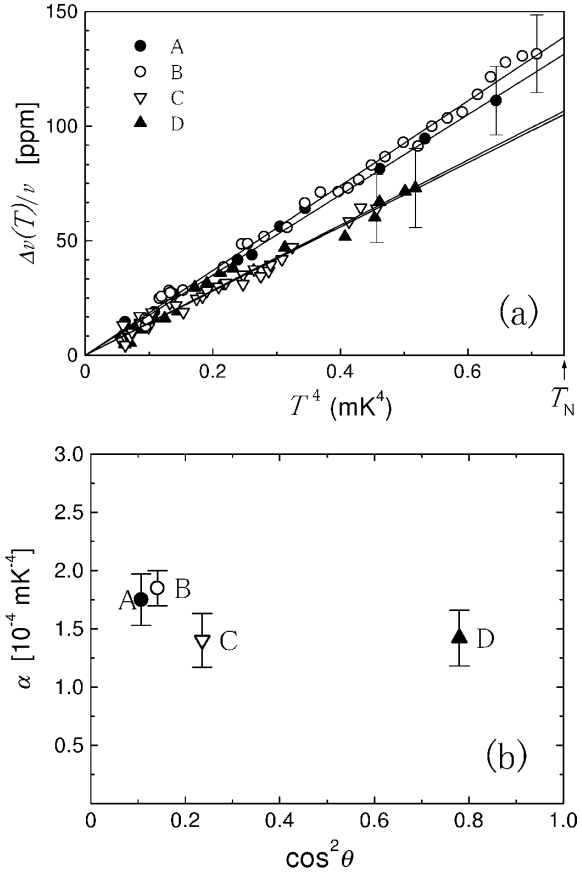

FIG. 3. (a) Temperature dependence of the sound velocity in the $U2D2$ phase for four different samples. (b) The coefficient, α, is plotted as a function of $\cos^2\theta$, where θ is the angle between $\mathbf{l}$ and the sound direction.

from the measured values of $\Delta v/v$. The contribution from the molar volume change is less than 20% in the $U2D2$ phase. Orientations of crystal with respect to sound propagation are indicated by a polar angle θ and an azimuthal angle ϕ where $\hat{\mathbf{z}}$ is chosen for the anisotropy axis $\mathbf{l}$ and $\hat{\mathbf{x}}$ and $\hat{\mathbf{y}}$ are (100) and other equivalent axes. They are tabulated in Table I. The coefficient of α, defined by $\Delta v(T)/v = \alpha T^4$, is plotted in Fig. 3(b) as a function of $\cos^2\theta$. It is known that the nuclear magnetic properties, such as NMR frequency shift, are very much isotropic in the plane perpendicular to $\mathbf{l}$ [5] and should be symmetric around $\mathbf{l}$, and thus the simplest functional form of $A + B\cos^2\theta$ is assumed for anisotropy of the temperature coefficient α. Anisotropy of α was found to be

TABLE I. Summary of anisotropy of sound velocity in the nuclear-ordered $U2D2$ phase. Sound directions $\{\theta, \phi\}$, velocities v, coefficient α, and Grüneisen constant for spin wave velocity γ_c are listed.

	$\{\theta, \phi\}$	v (m/s)	α	γ_c
A	$\{71°, 43°\}$	513	1.75 ± 0.22	17.0 ± 1.0
B	$\{68°, 39°\}$	514	1.85 ± 0.15	17.5 ± 0.7
C	$\{61°, 37°\}$	518	1.40 ± 0.23	15.5 ± 1.3
D	$\{29°, 28°\}$	489	1.42 ± 0.24	14.7 ± 1.2

$B/A \sim 0.1$. Fitting data to Eq. (5) together with Eq. (6), we can calculate γ which is related to the Grüneisen constant for spin wave velocity γ_c, as $\gamma = \gamma_c - \frac{1}{3}$. The values of γ_c are tabulated in Table I. The average value of γ_c for four samples is $\bar{\gamma}_c = 16$.

At T_N, the molar volume jump ΔV_{mol} is 2.14×10^{-3} cm^3/mole [13]. We estimate $\Delta v(V_{\text{mol}})/v$ to be about 0.02%. Entropy jump at T_N is reported to be $\Delta S = 0.49R \log 2$ [14] and $\Delta S = 0.43R \log 2$ [16], from which the internal energy jump is calculated. When the former value for ΔS is used, the observed value of the velocity jump of 0.1% at T_N gives $\gamma = 22$. Because of the long relaxation time in this temperature range an accurate estimate of the velocity jump is difficult. No orientation dependence was observed in velocity jumps within this accuracy.

In the paramagnetic phase above T_N, the free energy is given by the high-temperature series expansion of the nuclear spin system as

$$F = RT\left(-\frac{e_2}{8T^2} + \frac{e_3}{24T^3} - \ldots\right). \tag{7}$$

By fitting the internal energy calculated from the temperature dependence of melting pressure [17] to Eq. (7), we obtained $e_2 = 11.8$ mK^2 and $e_3 = 29.4$ mK^3 along the melting curve. As shown in Ref. [12], the adiabatic bulk modulus B_S is calculated by

$$B_S = B_T + \frac{T}{c_V}\left(\frac{\partial P}{\partial T}\right)_V^2, \tag{8}$$

where the isothermal bulk modulus, B_T, and heat capacity at constant volume, c_V, are calculated from Eq. (7). The nuclear spin exchange contribution to the sound velocity change is given by

$$\frac{\Delta v(T)}{v} = \frac{R}{2\rho v^2 V_{\text{mol}}}\left\{-\frac{e_2}{8T}\left(\frac{\gamma_2^2}{2} + \gamma_2 - \gamma_2\frac{d\log\gamma_2}{d\log V}\right) + \frac{e_3}{24T^2}\left(\gamma_3^2 + \gamma_3 - \gamma_3\frac{d\log\gamma_3}{d\log V} - 2\gamma_2\gamma_3 + \frac{3}{2}\gamma_2^3\right) - \cdots\right\}, \tag{9}$$

where $\gamma_2 \equiv \frac{d\log e_2}{d\log V}$ and $\gamma_3 \equiv \frac{d\log e_3}{d\log V}$. We assume $\frac{d\log\gamma_2}{d\log V} = 0$, and $\frac{d\log\gamma_3}{d\log V} = 0$ in Eq. (9). The dotted line in Fig. 2 is the contribution from molar volume change and the solid line is the fit to Eq. (3). For this sample we obtained $\gamma_2/2 = 21$ and $\gamma_3/3 = 22$. In the paramagnetic phase the main contribution to the sound velocity change is due to the molar volume

change along the melting curve and the accuracy in the estimation of γ_2 and γ_3 was poor. Indeed we found some samples where the above analysis did not fit well and the accuracy of the fit was marginal in the paramagnetic phase.

We compared $\bar{\gamma}_c = 16$ with that calculated by the multiple-exchange model [18]. We used the multiple-exchange frequencies calculated by the path integral Monte Carlo method of Ceperley and Jacucci [19]. We scaled those values to the molar volume on the melting curve using the Grüneisen constant, $\gamma = 18$, as done in TABLE III by Roger and Hetherington [20]. Grüneisen constants for various types of exchange processes are given by Roger [21] and Roger and Hetherington [20] in the form of $\gamma_p = \frac{5}{3}A_p/g$, where suffix, p, expresses the type of exchange, A_p is the action in the WKB calculation which is tabulated in their figures, and $g^{-1} = 1.1$. Spin wave velocity, c, was calculated by using multiple-exchange constants up to four-body exchange processes by Iwahashi and Masuda [22] and Ohmi *et al.* [23]. Using these values and expression for c, we obtained $c = 5.8 \pm 3.0$ cm/sec and $\gamma_c = 9.3 \pm 17.2$ where the errors came from stated errors of the Monte Carlo calculation in multiple-exchange constants [19]. Agreement with our experimental value, $\bar{\gamma}_c = 16$, is acceptable because spin wave velocity and its Grüneisen constant are very sensitive to the exchange frequencies. Comparison of the sound measurement with the theory would be a sensitive test for the multiple-exchange model, but an expression for spin wave velocity up to higher-order exchange processes than four-body exchanges and more accurate values of multiple-exchange constants are needed.

We measured the velocities of longitudinal sound in $U2D2$ solid ^{3}He in single-domain crystals with different orientations. Anisotropy of temperature dependent-sound velocity B/A was about 10% in the $U2D2$. Grüneisen constant for spin wave velocity, $\bar{\gamma}_c = 16$, was obtained. We compared this value with the multiple-exchange model up to four-body exchanges and the agreement was acceptable. The sound velocity jump at the first order phase transition and temperature dependence of sound velocity in paramagnetic phase were also explained by the contribution from the nuclear spin exchange process and the molar volume change along the melting curve.

We would like to thank H. H. Hensley, M. Suzuki, A. Uchida, and H. Shiga for their assistance in the early stage of this experiment. We also acknowledge useful discussions with H. Fukuyama, W. P. Halperin, T. Ishiguro, and T. Ohmi. Research was supported by the Ministry of Education, Science, Sports and Culture Grant-in-Aid for Scientific Research on Priority Area, and NEDO.

*Present address: Department of Condensed Matter Physics, Tokyo Institute of Technology, Meguro-ku, 152-8551, Japan.

[1] D. D. Osheroff, M. C. Cross, and D. S. Fisher, Phys. Rev. Lett. **44**, 792 (1980).
[2] M. C. Cross and D. S. Fisher, Rev. Mod. Phys. **57**, 881 (1985).
[3] A. Fartash and J. M. Goodkind, Phys. Rev. Lett. **56**, 1389 (1986).
[4] Y. Sasaki *et al.,* Phys. Rev. B **44**, 7362 (1991).
[5] Y. P. Feng, P. Schiffer, and D. D. Osheroff, Phys. Rev. Lett. **67**, 691 (1991).
[6] T. Matsushita *et al.,* J. Low Temp. Phys. **105**, 67 (1996).
[7] Y. P. Feng, P. Schiffer, D. D. Osheroff, and M. C. Cross, J. Low Temp. Phys. **90**, 475 (1993).
[8] Y. P. Feng, P. Schiffer, J. Mihalisin, and D. D. Osheroff, Phys. Rev. Lett. **65**, 1450 (1990); Y. P. Feng, P. Schiffer, and D. D. Osheroff, Phys. Rev. B **49**, 8790 (1994).
[9] R. Nomura *et al.,* J. Low Temp. Phys. **113**, 763 (1998); R. Nomura *et al.,* Physica (Amsterdam) **280B**, 140 (2000).
[10] D. S. Greywall, Phys. Rev. B **33**, 7520 (1986).
[11] D. S. Greywall, Phys. Rev. A **3**, 2106 (1971).
[12] R. Wanner, K. H. Mueller, Jr., and H. A. Fairbank, J. Low Temp. Phys. **13**, 153 (1973).
[13] W. Ni *et al.,* J. Low Temp. Phys. **100**, 167 (1995).
[14] D. D. Osheroff and C. Yu, Phys. Lett. **77A**, 458 (1980).
[15] Y. Okamoto, Physica (Amsterdam) **284B–288B**, 359 (2000).
[16] D. S. Greywall and P. A. Busch, Phys. Rev. B **36**, 6853 (1987).
[17] W. Ni *et al.,* J. Low Temp. Phys. **99**, 167 (1995).
[18] H. Fukuyama (private communication).
[19] D. M. Ceperley and G. Jacucci, Phys. Rev. Lett. **58**, 1648 (1987); **59**, 380 (1987).
[20] M. Roger and J. H. Hetherington, Phys. Rev. B **41**, 200 (1990).
[21] M. Roger, Phys. Rev. B **30**, 6432 (1984).
[22] K. Iwahashi and Y. Masuda, J. Phys. Soc. Jpn. **50**, 2508 (1981).
[23] T. Ohmi, M. Tsubota, and T. Tsuneto, Prog. Theor. Phys. **73**, 1075 (1985). There is a misprint of $c_\perp^2$ in Eq. (2.10). The correct one should be exactly the same as that in Ref. [22].